International Journal of Microwave and Wireless Technologies, 2016, 8(4/5), 795–805.
doi:10.1017/S1759078716000684

RESEARCH PAPER

UWB impulse radiation source with integrated optoelectronic generator

ROMAIN NÉGRIER[1], MICHÈLE LALANDE[1], VALÉRIE BERTRAND[2], JOËL ANDRIEU[1], VINCENT COUDERC[3], BADR M. SHALABY[4], LAURENT PECASTAING[5], ANTOINE DE FERRON[5] AND LAURENT DESRUMAUX[6]

This paper presents an innovative design of an Ultra Wide-Band (UWB) impulse radiation source. The transmitting system is composed of an UWB antenna with an integrated optoelectronic generator, which is able to feed the system with appropriate waveforms, a pulsed high voltage source, and an optical command system. The radiation source is the elementary part of a forthcoming short-range UWB Radar with autonomous scanning capability. In this paper, we present in detail the necessary subsystems required to design the elementary radiation source. Measurements have been performed to validate the proposed radiation source and this offers a mathematical method of calculation to trace back to the radiated field at 1 m.

Keywords: UWB antennas, Optical pulse generation, Optical switches

Received 12 October 2015; Revised 22 April 2016; Accepted 4 May 2016; first published online 31 May 2016

I INTRODUCTION

In multi-antennas transmitting system, the possibility of beamforming via employing optical delay has attracted a great interest over the years in the generation of radiated waveforms using optoelectronic devices [1–3]. The purpose is to provide an alternative to previous work in order to obtain a high-speed scanning system and presenting a more operational role with very short radiated waveforms, which is particularly crucial for short-range and through-the-wall detection applications.

Previous studies performed by XLIM and Centre d'Ingénierie des Systèmes en Télécommunications, Electro Magnétisme et Electronique (CISTEME) have already demonstrated the feasibility and advantages of a system combining as many antennas as optical generation devices, a "*n*" generators/"*n*" antennas architecture. The aforementioned type of architecture has been widely used for Ultra Wide-Band (UWB) synthetic aperture [4] and high power UWB radiation source applications [5].

The benefits of the previous demonstrators are relatively significant, especially in terms of shape control of the radiated waveform. It is also worth to note that the use of connectors and cables to connect the generator with the antenna introduces unnecessary electrical discontinuities. This will limit the performance of UWB radiation source, especially at high frequencies. In order to overcome this limitation, an integration of the optoelectronic generator has been simulated using a transient 3D EM/circuit co-simulation with CST Microwave Studio (MWS) and CST Design Studio (DS) [6–8].

The paper is organised as follows: Section II explains the design of an elementary radiation source, Sections III and IV respectively, introduce the pulsed high voltage source and the optical command. Measurements performed on the antenna with the integrated optoelectronic generator in order to validate the proper operation of the system are presented in Section V. In the same section, an analytical method is also proposed to build the radiated electrical field from the received signal and calibrations. Finally Section VI concludes the paper.

II. ELEMENTARY RADIATION SOURCE

The elementary radiator of the transmitting array consists of a UWB antenna and an integrated pulses generator, hence the name "elementary radiation source".

The optoelectronic generator, illustrated in Fig. 1, can deliver electrical short bipolar pulses by using the well-known frozen wave generator principle [9–11]. It is composed of a transmission line connected to the antenna via the first switch on the one end and a short-circuit via a second switch on the other end. Under fully loaded condition, the electrical energy stored in the 50 Ω microstrip line is released through the fast silicon photo-conductive switches, which can be activated by 80 ps optical pulse. The optical pulses are distributed to the photo-conductive switches via two optical fibres [6].

The photo-generated pulse shape can be easily modified by adjusting the parameters shown in Fig. 1, for example, the larger the optical energy on the switch A, the higher will be the magnitude of the positive half wave pulse generated. The

[1]XLIM/OSA Laboratory, University of Limoges, Brive-la-Gaillarde, France
[2]CISTEME, Limoges, France
[3]XLIM/PHOTONIQUE Laboratory, University of Limoges, Limoges, France
[4]Physics Department, Faculty of Science, Tanta University, Egypt
[5]SIAME Laboratory, University of Pau, Pau, France
[6]DGA, Paris, France
Corresponding author:
R. Négrier
Email: romain.negrier@xlim.fr

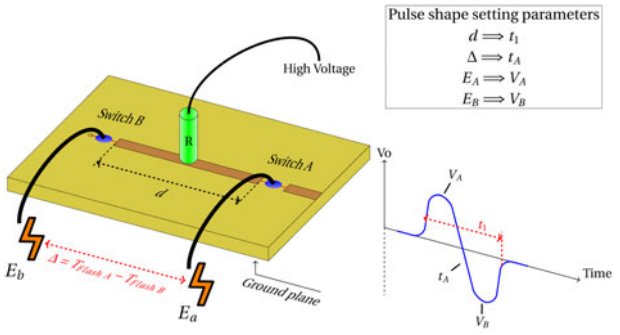

Fig. 1. Generator with tunable parameters and photo-generated pulse shape.

parameters are selected accordingly so that the spectrum of the generated pulses matches with the adaption band of the antenna. This will ensure the minimum standing waves generated between the edge of the antenna and the supply device.

The UWB antenna chosen for this application has been inspired by the radiator developed by Koshelev [12], which combines a magnetic loop and the radiation mode of a travelling wave antenna. The polytétrafluoroéthylène (PTFE) (Teflon) part added below the feeding point enables high voltage applications. Indeed, to reach high voltage levels we rather used a microstrip line, thus preventing undesired breakdown between the line and the ground. The simulation model and the antenna prototype with an integrated photoswitch can be seen respectively, in Figs 2(a) and 2(b). The model of the photoswitch is detailed in [6].

Figure 3 shows the simulation results obtained for the elementary radiation source using CST MWS. The simulation has been performed by feeding the embedded optoelectronic generator antenna with a photo-generated pulse using a waveguide port at the intersection of the transmission line and the beginning of the flare part. With a length of around 30 cm, a height of 21 cm, and a thickness of 10 cm, this antenna has a very wide adaptation (−10 dB) with a matching bandwidth between 0.3 and 3 GHz (Fig 3(a)). Figure 3(b) shows that the realized gain in the main radiation direction is low for frequencies under 1 GHz and moderate/high for frequencies above 1 GHz. Radiation patterns of antennas in *E* and *H* planes are also respectively shown in Figs 3(c) and 3(d), to give an idea of the evolution of half power beam width with respect to frequency.

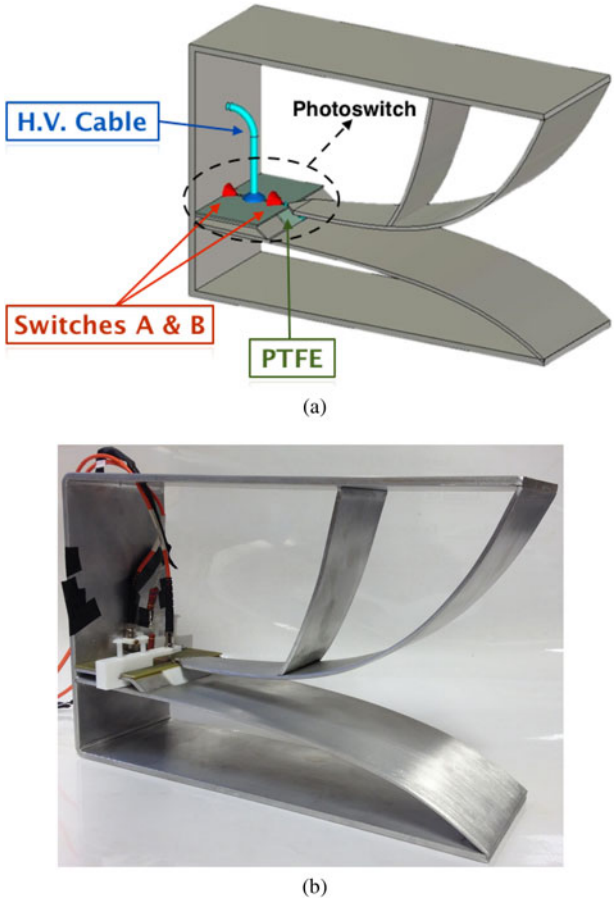

Fig. 2. (a) CST model and (b) prototype of the elementary radiation source composed of the photoswitch and the UWB antenna.

III. THE PULSED SOURCE

The lifetime of the photoswitches A and B (Fig. 2(a)) normally depend on the duration of the high voltage applied. So it is essential to drive optical switches using a pulsed voltage. In this context, Sciences pour l'Ingénieur Appliquée à la Mécanique et au génie Electrique (SIAME) laboratory has designed and realized a pulsed power source, which is able to control both the amplitude and the bias voltage of the photoconductive switches.

The DC source (Fig. 1-*High Voltage*) used to polarize photoswitches has been replaced by a pulsed source and this leads to an increase in the maximum voltage switched by photodiodes and as a consequence, a better performance for the radar. The pulsed voltage waveform applied to the photoswitches must be a high voltage square pulse in order to polarize the generator during several switchings (15 pulses applied to the antenna) with a very low drop. The main characteristics of pulsed power source are:

- Maximum output voltage = 12 kV
- Load = 10 pF, mainly due to microstrip line between switches
- Pulse width = 450 ns
- Pulse repetition frequency of a few tens of Hz
- No significant drop during the pulse.

To meet the above mentioned criteria, the choice has been made to use insulated gate bipolar transistors (IGBTs) technology, whose characteristics such as the rise time, the jitter and the repetition frequency are consistent with our problem. A series components association enables high switching performances, rather than using a single component and uses low calibre semiconductors to keep significant speed performances (the speed of the series arrangement can be the same of each of its components).

Figure 4 shows the schematic diagram of the pulsed source. A series combination of 14 IGBTs, knowing that each IGBT can withstand 1.2 kV, can support 16.8 kV, offers the flexibility of achieving the maximum required voltage of 12 kV. The 14 switching components must be turned-on simultaneously to obtain a steady and relatively fast rise-time.

This particular arrangement allows a very weak value of the stray inductance of the high voltage part and prevents undesired breakdown on the circuit surface, thanks to a sufficient distance between high and low voltage parts. In these conditions, the pulsed power source is able to generate the output voltage as

https://doi.org/10.1017/S1759078716000684 Published online by Cambridge University Press

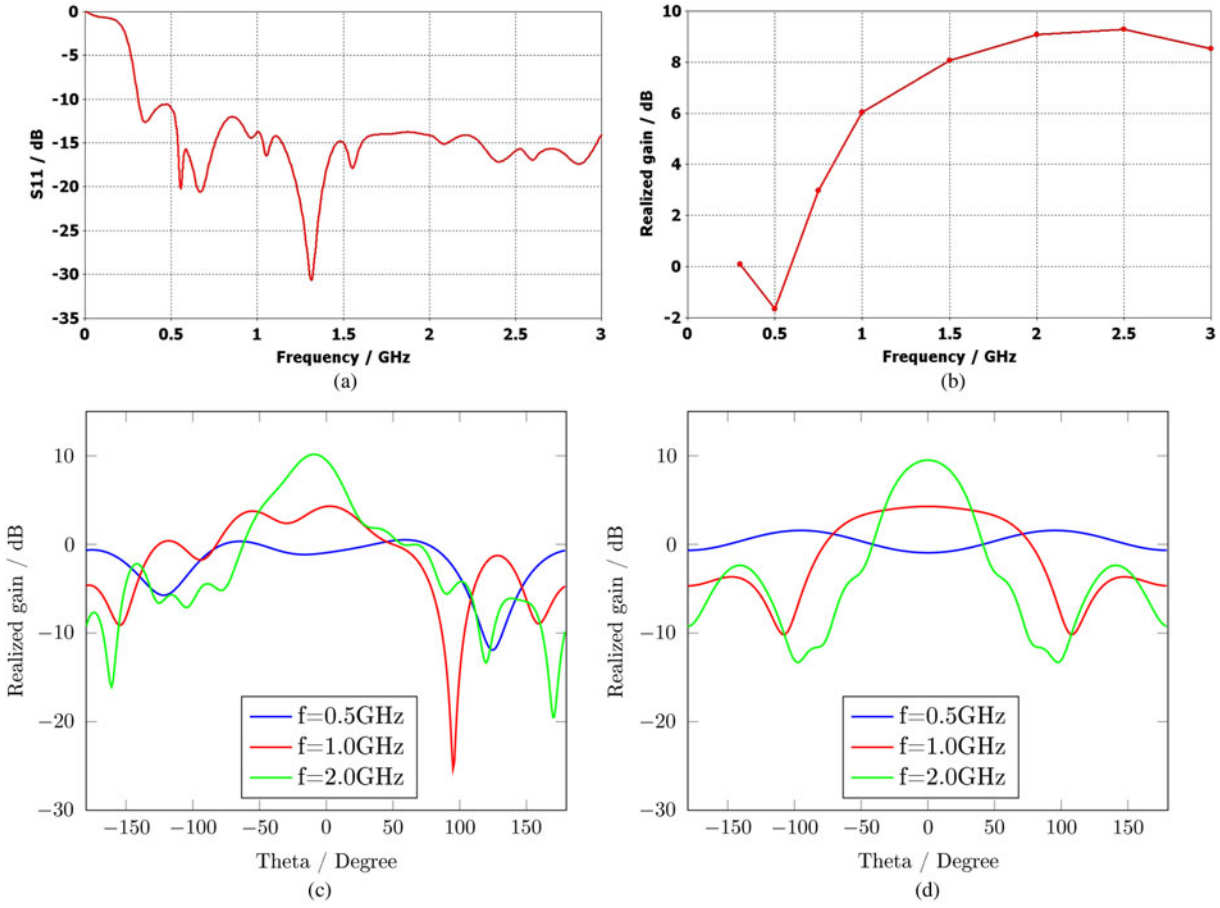

Fig. 3. Reflection coefficient (a), realized gain in the main direction for the antenna with integrated photoswitch (b), radiation patterns for *E* (c) and *H* (d) planes.

shown in Fig. 5-*yellow curve*. The maximum voltage obtained is 12 kV, with its rise-time and pulse width of 150 ps and 450 ns.

IV. THE OPTICAL COMMAND

The most adequate optical sources capable of realizing the optical control are the mode locked lasers combined with a pulse picker and an amplification stage in a regenerative amplifier. In this application, a pulsed Nd:YAG/CR4+:YAG microchip laser source has been used to realize the optical command as depicted in Fig. 6. This laser delivers 500 ps pulses in the infrared domain at 1064 nm. The output pulse energy is coupled with a 40 m long optical fiber in order to adjust an optical delay, enabling the synchronization between the microchip laser and the regenerative amplifier. The regenerative amplifier is composed of two Pockels cells, two polarizers and a Nd:YAG rod integrated in 1.8 m long optical cavity.

Nonlinear rotation of the pulse polarization due to the propagation in optical fiber is filtered by the polarizer P_1, which

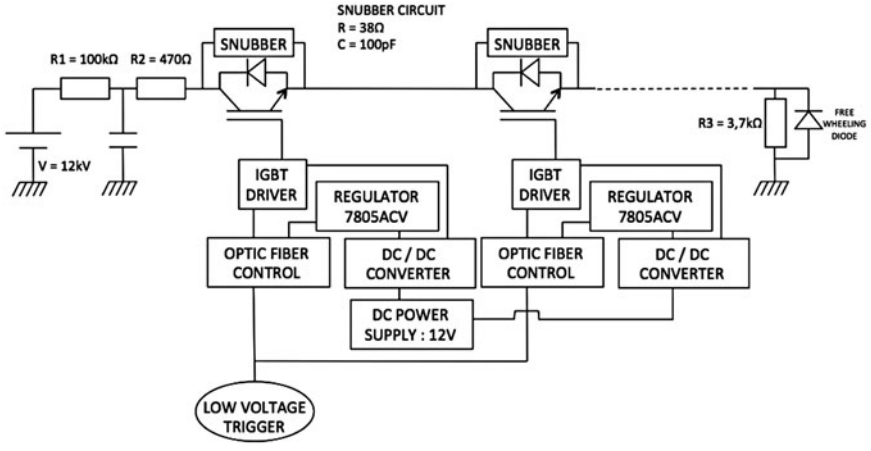

Fig. 4. Schematic diagram of series-connected IGBTs combination.

https://doi.org/10.1017/S1759078716000684 Published online by Cambridge University Press

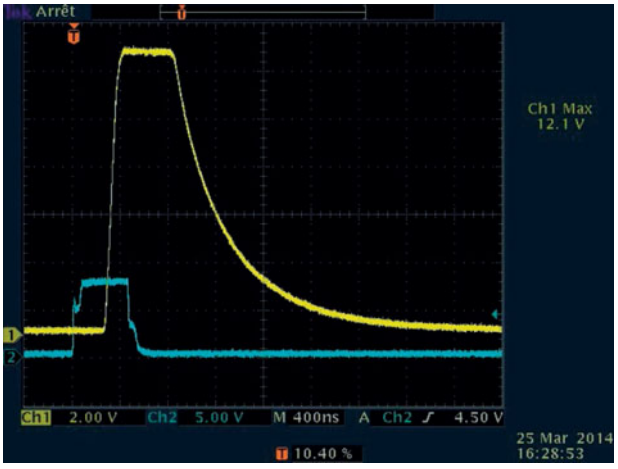

Fig. 5. Experimental result obtained with 14 series-connected IGBTs – CH1: HV signal with $V_{out} = 12$ kV (Attenuator = 60 dB) and CH2: low voltage trigger.

induces pulse shortening before the amplification step. A time profile of the reshaped optical pulse is shown in Fig. 7(a).

To obtain an ultrafast pulse train in the MHz range, a Pockels cell is activated in order to release a part of the pulse energy, which oscillates in the regenerative cavity. This process is maintained during several hundreds of nanoseconds to obtain a train of pulses. The length of the amplifier imposes the output repetition rate. Cavities longer than tens of meters have been already demonstrated (repetition rate <4 MHz) [13]. Here, the output repetition rate (33.8 MHz) is fixed by the frequency round-trip of the pulse in the regenerative amplifier and the number of pulses constituting the train is controlled by the open-time of the second Pockels cell.

The optical system is able to generate either a single monopolar(only one photoswitch is illuminated)/bipolar(both of the switches are illuminated) pulse (Fig. 7(a)) or a monopolar/bipolar pulse train (Fig. 7(b)). The maximum energy per pulse is set to 25 μJ.

V. MEASUREMENT

In this section, radiation measurements in the main direction have been performed to control the operation of the complete source combining the antenna with the integrated optoelectronic generator, the laser source, and the pulsed bias source. Initially, we focus on the impact of the probe on radiation to avoid any undesired disturbances. Then, we discuss the main results obtained in different configurations in terms of pulse shape and bias level. We also introduce a propagation model used to rebuilt the radiated electrical field in the main direction of the transmitting antenna.

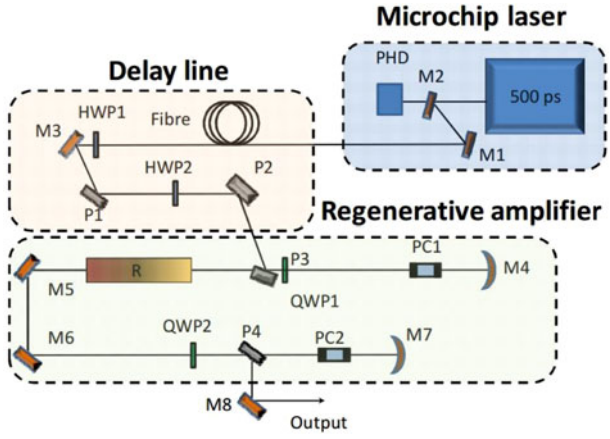

Fig. 6. Optical system – PC: pockels Cell; HWP: half wave plate; QWP: quarter wave plate; R: rod; M: mirror; PHD: PHotoDiode.

A) Experimental setup

The experimental configuration depicted in Fig. 8(a), describes the main settings and references of the material used.

The optical source is installed on an optical table (Fig. 8(d)) in a measurement room. The pulsed bias source (Fig. 8(e)) is located near the optical source. The antenna with the embedded photoswitch (Fig. 8(b)) is placed on a physical support and the receiving antenna is located in front of the transmitting antenna. The receiving antenna (Fig. 8(c)) is a K-antenna with a bandwidth at −10 dB of 300 MHz–3 GHz. The distance between antennas is 5.17 m and positioning height is 2.45 m. The voltage in the transmitting antenna (or just after the optoelectronic generator at the beginning of the flare part) is measured with the oscilloscope through a high voltage probe (Fig. 8(b)). The used probe (Barth 2440–6 GHz of Electronic Technology) is specific for the measurement of high voltage short pulses (up to 5 kV and up to 60 ps rise time). This probe has an input resistance of 1 kΩ on a 50 Ω load and provides 1/20 of the measured voltage (26 dB). The advantage of using this voltage probe is to facilitate the optical adjustments. The reception voltage is measured directly on the oscilloscope through a 26 dB attenuator to protect it from unexpected high power fluctuations. The oscilloscope used is a digital real-time oscilloscope (model: DSO-X92004Q) from Agilent Technologies with a bandwidth of 20 GHz.

The oscilloscope operates in interpolated mode with a sampling rate of 80 Gsa/s. Measurements are recorded after a 64 pulses averaging. The trigger mode is edge trigger on either the signal from the voltage sensor placed in the issuing or directly from the voltage measured with the receiving antenna.

Table 1 summarizes the main characteristics of the most significant radiation measurements. A first series of measurements was carried out using low-level DC bias voltage to check the influence of the voltage probe on the receiving voltage. The DC bias level has been increased to 1 kV. The DC bias source was then replaced with the pulsed voltage source; tests were conducted to photogeneration of a single pulse (SP) and a burst composed of 20 pulses. Depending on the number of illuminated photoswitches (one or two), two shapes have been photogenerated: monopolar (mono) and bipolar (bi). The load resistance has been welded in the middle of the transmission line in order to easily adjust the RC charging time constant. Several configurations have been tested to find out a good trade off for the load resistance value. This value should not be too low to avoid the back propagation into the high voltage cable and should not be too high to allow a loading time of the line shorter than the repetition rate in burst mode. T_x corresponds to the measurement of the photogenerated signal via the probe and R_x corresponds to the signal measured using the receiving antenna.

https://doi.org/10.1017/S1759078716000684 Published online by Cambridge University Press

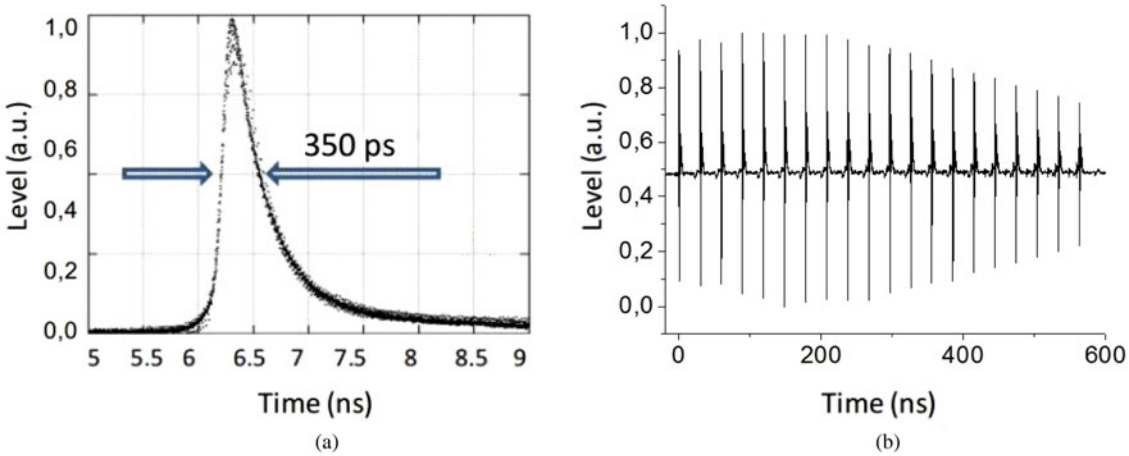

Fig. 7. Monopolar pulse shape after temporal shortening (a), bipolar pulses train at 33.8 MHz (b).

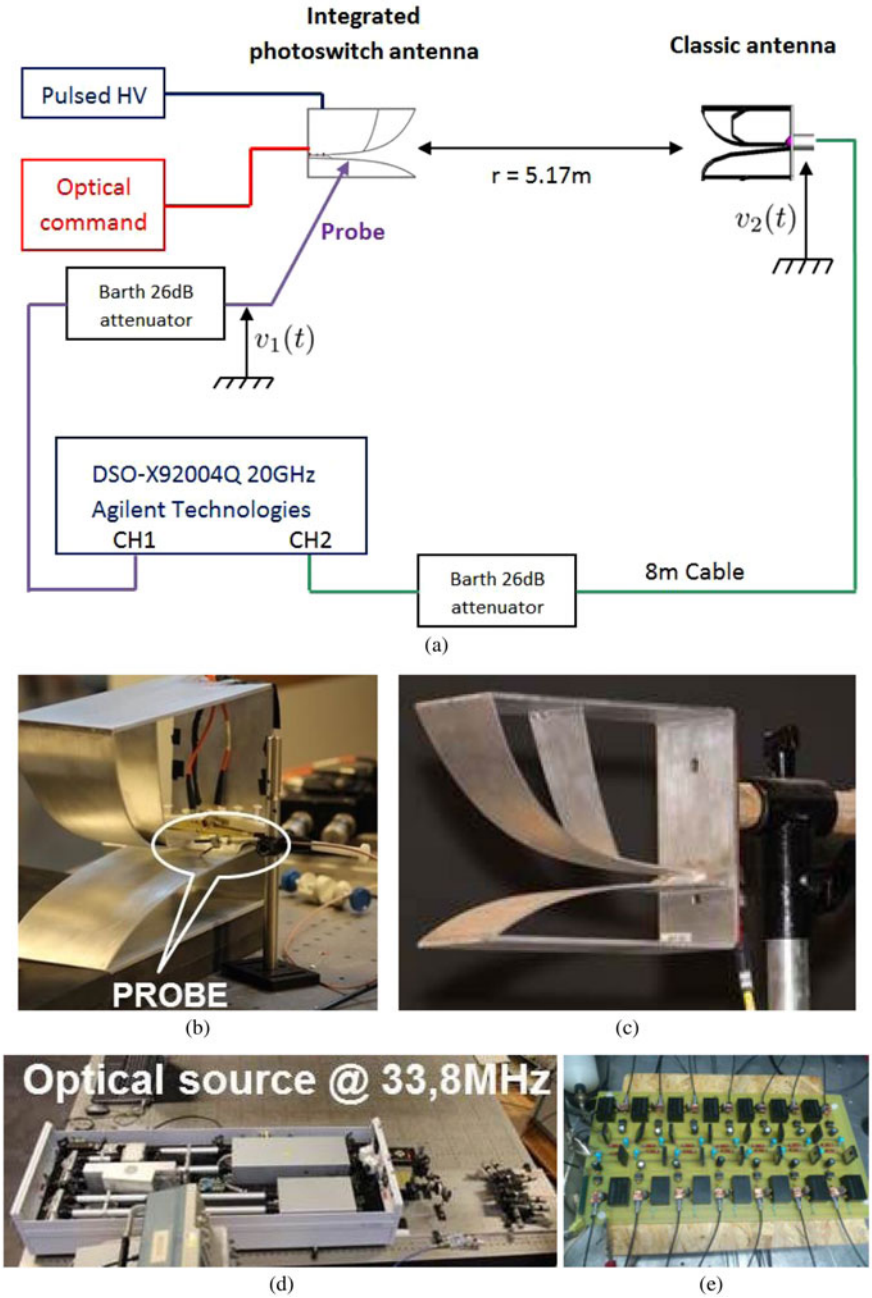

Fig. 8. Experimental setup schematic layout (a), probe (b), receiving antenna (c), optical command (d), pulsed high voltage source (e).

https://doi.org/10.1017/S1759078716000684 Published online by Cambridge University Press

Table 1. Radiated measurements features.

	T_x	R_x	Bias mode	Bias level/kV	Load res./ kΩ	Shape	Waveform
1	☑	☑	DC	0.15	1.87	bi	SP
2	☑	☑	DC	0.15	1.87	mono	SP
3	☐	☑	DC	0.15	1.87	bi	SP
4	☐	☑	DC	0.15	1.87	mono	SP
5	☐	☑	DC	1	1.87	bi	SP
6	☐	☑	DC	1	1.87	mono	SP
7	☑	☑	Pulsed	1	1.42	bi	SP
8	☑	☑	Pulsed	1	1.42	mono	SP
9	☐	☑	Pulsed	1	1.42	bi	Burst
10	☐	☑	Pulsed	1	1.42	mono	Burst
11	☑	☑	Pulsed	1	0.1	bi	Burst
12	☑	☑	Pulsed	1	0.1	mono	Burst

B) Measured voltage

1) MEASUREMENTS 1–4

Figure 9(a) shows the voltage in the antenna measured by the probe. The voltage levels correspond to a correction of 52 dB (26 dB attenuator and 26 dB probe). The optical adjustments have been optimized for the photogeneration of a bipolar pulse.

The measured voltage is a bipolar shape followed by some characteristic oscillations of the signal reflected at the edge of the antenna. The peak to peak level of the voltage is 64.5 V for a 150 V bias.

The voltages measured at the receiving antenna output with or without the probe voltage are compared in Fig. 9(b). The presence of the probe does not interfere with the radiated field in the main direction. Indeed, the transient shapes are similar (derived from the bipolar) and the peak to peak levels are slightly higher when the voltage sensor is removed.

The same experiment has been performed for the generation of a monopolar pulse. The voltage measured at the output of the probe has a steep rising edge followed by strong oscillations with low frequency content reflected at the edge of the antenna (Fig. 9(c)). These oscillations are caused by the mismatch between the spectrum of the monopolar pulse (which starts from DC) and the antenna bandwidth. This observation highlights the advantage of using bipolar pulses rather than monopolar pulses [6, 14, 15]. The peak voltage level of 77 V is obtained for an input voltage bias of 150 V.

As the generation of the bipolar pulse, we consider that the presence of the probe does not disturb the radiation in the main axis (Fig. 11). Therefore, these results confirm the

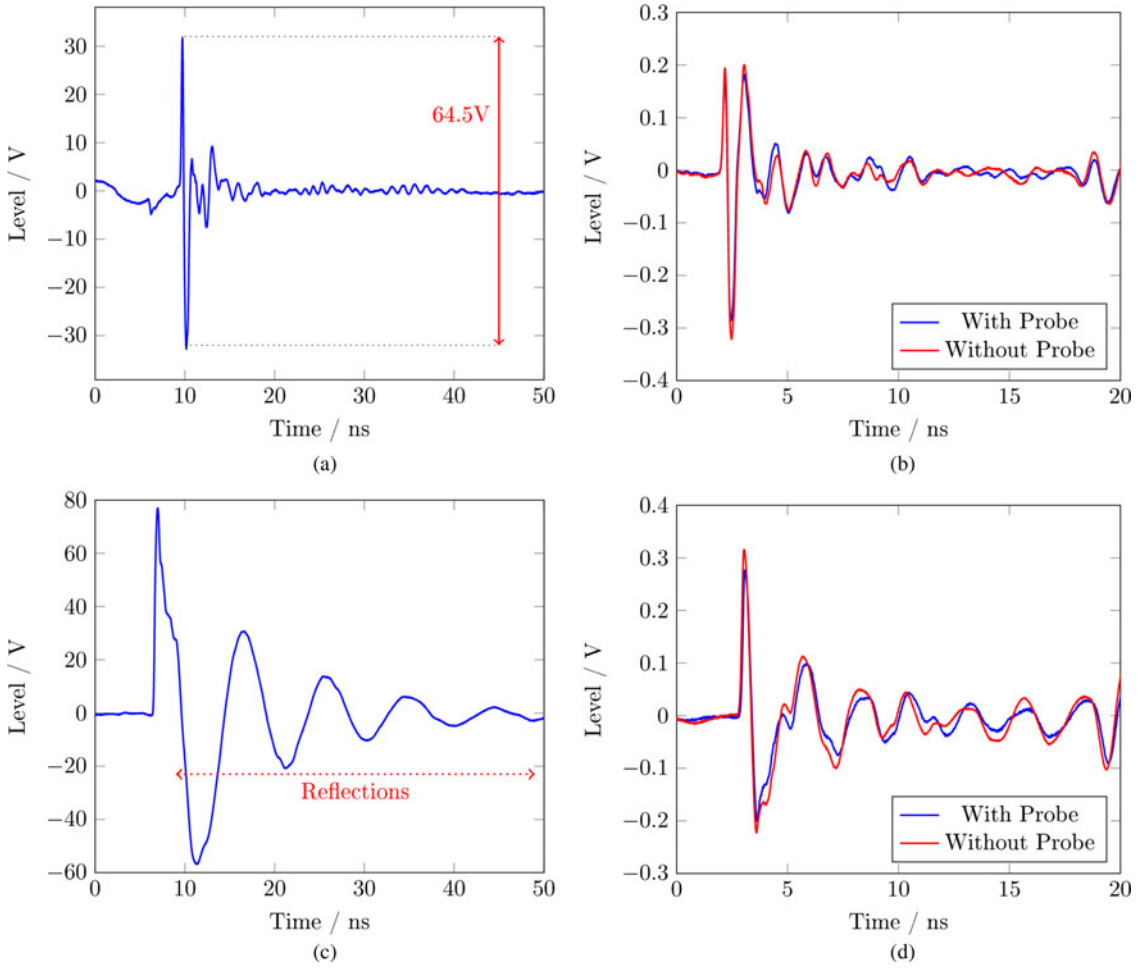

Fig. 9. (a) Probe measurement with a correction of 52 dB – bipolar shape, (b) received signals on the antenna with a correction of 26 dB with and without the probe for a bipolar shape, (c) probe measurement with a correction of 52 dB – monopolar shape, and (d) received signals on the antenna with a correction of 26 dB with and without the probe for a monopolar shape.

https://doi.org/10.1017/S1759078716000684 Published online by Cambridge University Press

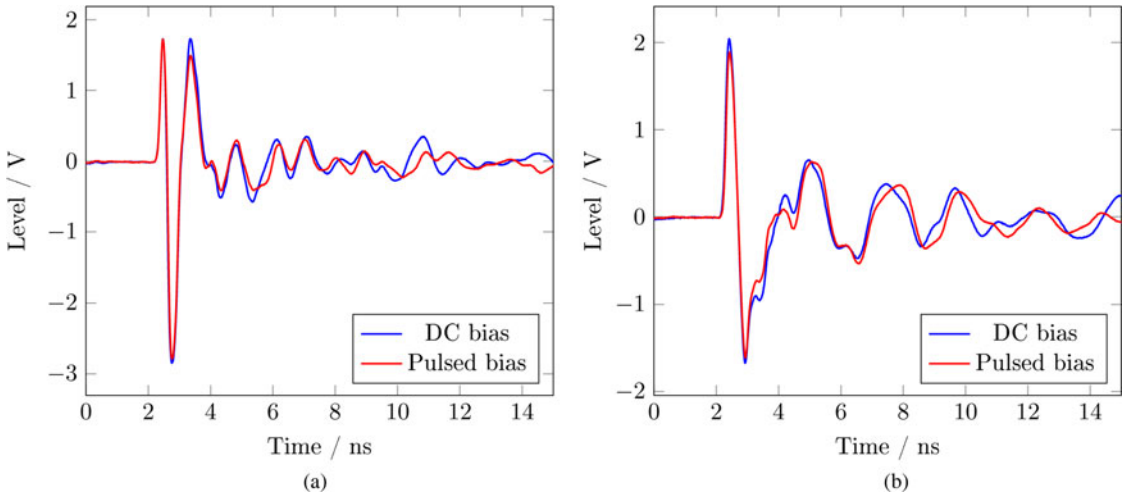

Fig. 10. Received signals on the antenna with a correction of 26 dB for (a) a bipolar shape and (b) a monopolar shape – DC and pulsed bias correspond respectively, to the blue curve and the red curve.

possibility of using this probe to optimize the settings of the optical beam needed for the photogeneration.

2) MEASUREMENTS 5 AND 6

For measurements 5 and 6, a DC bias voltage of 1 kV is applied. The transient shapes of these voltages are comparable with previous ones (Figs 9(b) and 9(d)).

The energy yield, which can be defined as the ratio between the output level of the photogenerated pulse and the bias voltage for the same optical power, is better in the case of a bipolar signal (Fig. 10(a)). Intuitively, this is entirely consistent and comes from a better compatibility between the spectrum of the bipolar pulse and the antenna frequency response. Furthermore, increasing the voltage level for a monopolar signal corresponds to the ratio 1 kV/150 V (Fig. 10(b)).

3) MEASUREMENTS 7 AND 8

The DC bias source have been replaced by the pulsed voltage source developed by SIAME laboratory as described earlier in this paper (Section III). The configuration is the same as the ones used for the measurements 5 and 6 with 1 kV level bias in SP mode. The transient shapes and measured voltage are very close whatever the bias mode (10).

4) MEASUREMENTS 9 AND 10

Measurements 9 and 10 have been performed in the same configuration in terms of bias level with the generation of a burst composed by 20 bipolar pulses at 33.8 MHz. Figure 11(a) shows the received signal with a bipolar pulses burst and a monopolar pulses burst 11(b). The period between each pulse is stable and is equal to 29.59 ns.

The consistency between the pulse amplitudes obtained at the output of the system is not perfect. This distortion is directly attributable to the atypical features of the source and more precisely to the changes in the laser gain along the multipass cavity. In Fig. 11(b) we can notice strong oscillations between two successive pulses and this is owing to the low frequency content, which is not radiated by the antenna. A comparison has also been performed between the magnitude of a SP and the magnitude of a pulse contained in a burst. The SP

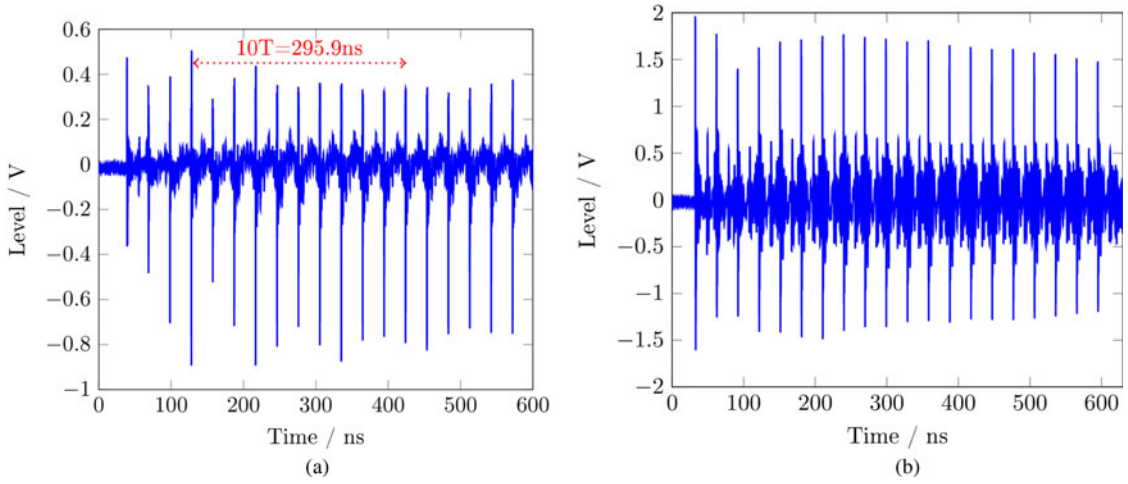

Fig. 11. Received signal for a bipolar pulses burst (a) and a monopolar pulses burst (b) with 1 kV pulsed bias level and 1.42 kΩ load resistor.

https://doi.org/10.1017/S1759078716000684 Published online by Cambridge University Press

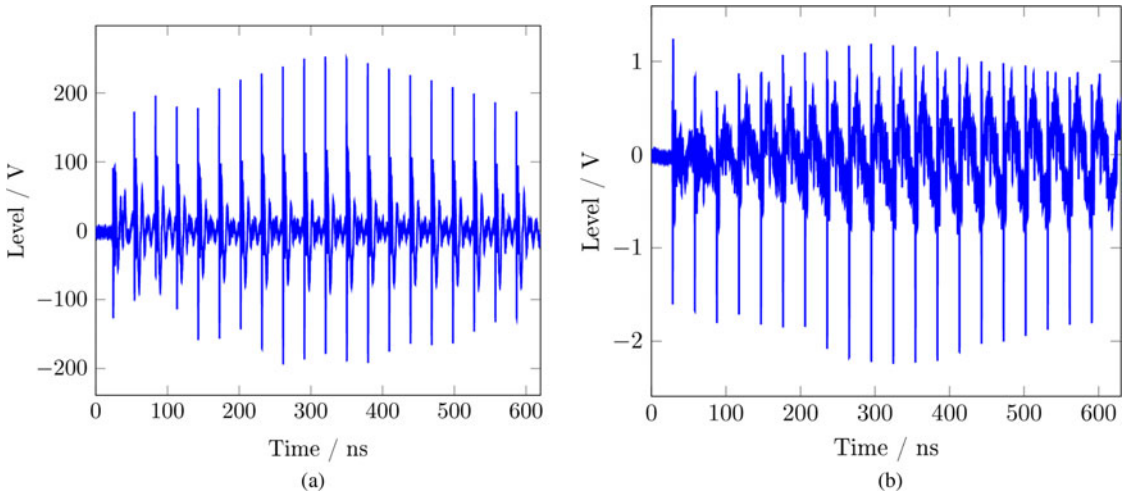

Fig. 12. Probe measurement (a) and received signal (b) for a bipolar pulses burst with 1 kV pulsed bias level and 100 Ω load resistor.

is 3.2 times higher than the pulse contained in a burst, because the optical power voluntarily decreases to take into account the recovery time of optical switches, to ensure that the diode has enough time to return to the off state.

5) MEASUREMENTS 11 AND 12

For the last measurements, the load resistor 1.42 kΩ has been changed by a 100 Ω resistor. The voltage measured with the probe is shown in Fig. 12(a) for the photogeneration of bipolar pulses. The photogenerated pulses amplitude changes significantly. The average peak to peak magnitude is around 400 V for a 1 kV bias voltage.

Figure 12(b) shows the received pulse train. The level of the pulses changes in accordance with variations in the amplitude of photogenerated pulses. The maximum peak to peak level is higher (3.4 V) than for the measurements done with a load resistor 1.42 kΩ (1.1 V). The decrease in loading time of the line enhances performance. However, the oscillations between two pulses are stronger. These spurious signals are introduced by the pulsed bias source, with a lower load resistance, more energy may be coupled on the transmission line for the recovery of the semiconductor insulation characteristics.

Measurement 12, presented in Fig. 13 shows that the amplitude variations are significant for the first pulses and the average peak level is 700 V. The corresponding measured signal reception showed an average level of 4.5 V peak to peak, which is much stronger than the measurements obtained with a 1.42 kΩ load resistance. As before, the yield is improved but the oscillations between two pulses are significant.

C) Radiated field at 1 m

A propagation model has been developed to estimate the photogenerated radiated field at a distance of 1 m using the signal measured at the receiver. Indeed, this model takes into account the receiving antenna, cables, and attenuator transfer functions. Deduced from the Friis formula, we can easily demonstrate the equation (1).

$$\underline{E}_{1m}(f) = \underline{V}_2(f) \cdot \frac{r}{\underline{H}_r(f).\underline{H}_l(f)}, \tag{1}$$

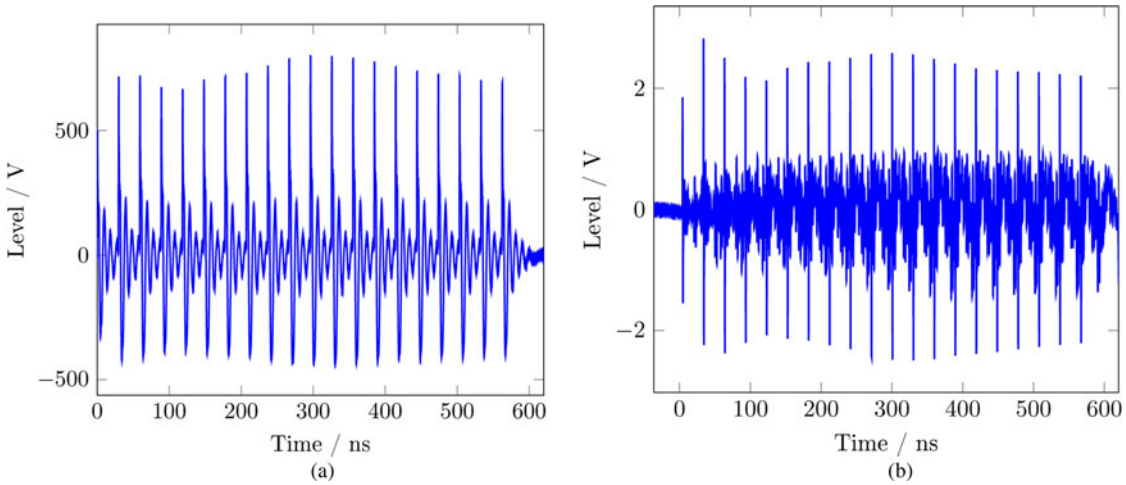

Fig. 13. Probe measurement (a) and received signal (b) for a monopolar pulses burst with 1 kV pulsed bias level and 100 Ω load resistor.

https://doi.org/10.1017/S1759078716000684 Published online by Cambridge University Press

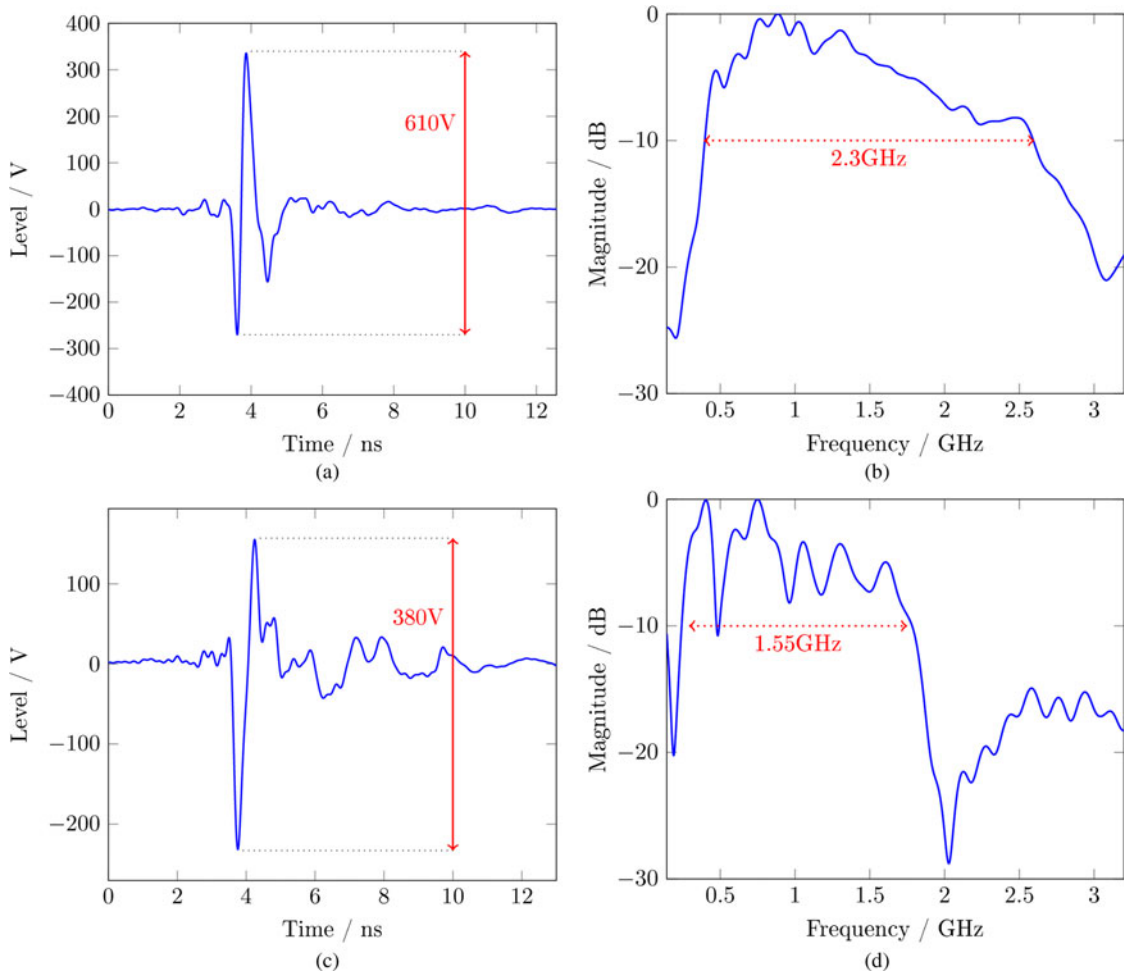

Fig. 14. Radiated field at 1 m (a) transient shape $e_{1m}(t)$ for a bipolar pulse (a) – monopolar pulse (c) and spectrum of the bipolar pulse (b) – monopolar pulse (d).

with:

- $\underline{E_{ph}}(f)$, Fourier transform complex notation of the photogenerated radiated field at 1 m $e_{1m}(t)$
- $\underline{V_2}(f)$, Fourier transform complex notation of the measured voltage on receiving antenna $v_2(t)$
- $\underline{H_r}$, transfer function complex notation of the receiving antenna
- $\underline{H_l}$, transfer function complex notation representing losses (attenuator and cable)
- r, distance between the receiving antenna and the transmitting antenna.

$\underline{H_r}$ and $\underline{H_l}$ has been computed using measurements previously performed to characterized receiving antenna, cables, and attenuator.

This calculation has been applied to the measurements 7 and 8 for which the pulsed bias source is set to 1 kV. The peak to peak level of the electric field at 1 m is 610 V for the photogeneration of a bipolar signal (Fig. 14(a)) and 380 V for a monopolar signal (Fig. 14(c)) and the spectrum of bipolar radiated signal is wider (Fig. 14(b), BW at −10 dB: 350 MHz–2.65 GHz) than the monopolar signal (Fig. 14(d), BW at −10 dB: 250 MHz–1.8 GHz).

The yield in this case is better than for the previous tests (150 V of DC bias level). The figure of merit, which can be defined as the ratio between the maximum amplitude of the radiated field at 1 m and the amplitude of the feeding pulse, is 1 for bipolar pulse and 0.8 for monopolar pulse. These values are low but depend on the photogenerated spectrum signals. Indeed, for a photogenerated pulse whose spectrum extends to 3 GHz, the theoretical factor of merit of the antenna is 1.6.

VI. CONCLUSION

In this paper, an innovative optoelectronic system capable of generating picoseconds kilovolt pulses with a repetition rate higher than tens MHz has been presented. First, we described a new kind of UWB elementary radiation source with an integrated photoswitch triggered by optical flash. Measurement result validates the operation of the complete radiation source with the generation and the radiation of bursts composed of 20 pulses at a frequency 33.8 MHz. The levels of radiated electric fields are consistent with the expected results. The radiated spectrum of the monopolar electrical signal generated is mainly composed of low frequencies and does not cover a frequency band up to 3 GHz, which is perfectly understandable and expected as long as the monopolar pulse shape is not suitable with the used K-antenna. The

https://doi.org/10.1017/S1759078716000684 Published online by Cambridge University Press

shaping of the pulse using bipolar signal would precisely control the spectrum around the central frequency and enhance the desired bandwidth. It is therefore shown that perfectly matching the profile of the spectrum related to the signal and the one related to the spectral characteristics of the antenna allows to optimize the radiation system. Finally, the integration of the optoelectronic source enhances the compactness of the system and would be even more interesting if the frequency band is higher.

ACKNOWLEDGEMENT

This work was supported by the French armament procurement agency DGA and the French National Research Agency ANR.

REFERENCES

[1] Rotman, R.; Raz, O.; Barzilay, S.; Rotman, S.R.; Tur, M.: Wideband antenna patterns and impulse response of broadband RF phased arrays with RF and photonic beamforming. IEEE Trans. Antennas Propag., **55** (1) (2007), 36–44.

[2] Bratchilov, A.N.: Photonic beamforming in ultra-wideband phased antenna arrays: present state and perspectives, in Ultrawideband and Ultrashort Impulse Signals, Sevastopol, Ukraine, 19–22 September 2006, 159–164.

[3] Lee, J.J.; Livingston, S.; Loo, B.; Jones, V.; Foster, C.: Performance of an optically fed conformal array, in Antennas and Propagation Society Int. Symp., vol. **2**, 1994, 828–831, Digital Object Identifier:10.1109/APS. 1994.407964.

[4] Lalande, M. et al.: An ultra wide band impulse optoelectronic radar: RUGBI. Prog. Electromag. Res. PIER B, **11** (2009), 205–222.

[5] Desrumaux, L.; Godard, A.; Lalande, M.; Bertrand, V.; Andrieu, J.; Jecko, B.: An original antenna for transient high power UWB arrays: the shark antenna. IEEE Trans. Antennas Propag., **58** (8) (2010), 2515–2522.

[6] Bertrand, V. et al.: Equivalent model of photoswitch: application to the UWB antenna design integrating impulse feeding. Prog. Electromag. Res. C, **46** (2014), 145–151.

[7] Négrier, R. et al.: UWB antenna array with autonomous scanning capability using opto-electronic feeding device, in Int. Conf. on Antenna Measurements and Applications – Focus on Antenna Systems, Antibes – Juan-Les-Pins, France, 16–19 November 2014.

[8] Négrier, R.; Bertrand, V.; Lalande, M.; Andrieu, J.; Couderc, V.; Pecastaing, L.; Ferron, A.D.: Improvement of an UWB impulse radiation source by integrating photoswitch device, in European Radar Conf. 2014, Fiera di Roma – Rome, Italy, 5–10 October 2014.

[9] Nunnally, W.: High-power microwave generation using optically activated semiconductor switches. IEEE Trans. Electron Devices, **37** (12) (1990), 2439–2448.

[10] Riaziat, M.L.; Nishimoto, C.K.: Compact optically triggered microwave pulse generator. Microw. Opt. Technol. Lett., **5** (5) (1992), 211–215.

[11] Best, S.; Rose, M.; Shotts, Z.; Rader, M.; Altgilbers, L.: Frozen Wave Generator technology as a source of constant amplitude high power high frequency radio frequency pulses, in 2013 19th IEEE Pulsed Power Conf. (PPC), San Francisco, CA, June 2013, 1–6.

[12] Koshelev, V.; Buyanov, Y.; Andreev, Y.; Plisko, V.; Sukhushin, K.: Ultrawideband radiators of high-power pulses. Pulsed Power Plasma Sci. 2001 Digest Tech. Papers, **2** (2001), 1661–1664.

[13] Gerhard, C.; Druon, F.; Georges, P.; Couderc, V.; Leproux, P.: Stable mode-locked operation of a low repetition rate diode-pumped Nd: $GdVO_4$ laser by combining quadratic polarisation switching and a semiconductor saturable absorber mirror. Opt. Express, **14** (16) (2006), 7093–7098. [Online]. Available: https://hal.archives-ouvertes.fr/hal-00127373

[14] Kardo-Sysoev, A.: Generation and radiation of uwb-signals, in Microwave Conf., 2003 33rd European, Munich, Germany, October 2003, 845–848.

[15] Diot, J.-C. et al.: Impulse optoelectronic ultra-wide band antenna array, in 2006 First European Conference on Antennas and Propagation, Nice, France, November 2006, 1–6.

Romain Négrier received the Dipl.-Ing. degree in mechatronics from the Engineers School of Limoges, Limoges, France, in 2012. He is currently pursuing the Ph.D. degree from the XLIM Laboratory, University of Limoges, Limoges, France. For nearly a year, he worked as a Research Engineer with the High-Power Microwaves Department, CEA, Gif-sur-Yvette, France, which is a French government-funded technological research organization. His research interests include the development of ultrawideband RADAR system and the associated images processing.

Michèle Lalande received the Ph.D. degree in electronics from the University of Limoges, Limoges, France, in 1986. She is currently a Professor with the University of Limoges and a Member of XLIM Research Institute, University of Limoges/National Center for Scientific Research (CNRS), Brive, France. Her research interests include the area of antennas and transient measurement applications and ultrawideband metrology for various applications: radar and HPMs.

Valérie Bertrand was born in Bellac, France, in 1970. She received the Ph.D. degree in electronics from the Université de Limoges, Limoges, France, in 1996. She is currently an Engineer with the Centre d'Ingénierie des Systèmes en Télécommunication, ElectroMagnétisme et Electronique, Ester, France. She is involved in the field of optoelectronic device conception and antennas and transient applications, such as radar and high-power microwaves.

https://doi.org/10.1017/S1759078716000684 Published online by Cambridge University Press

Joël Andrieu received the Ph.D. degree in electronics from the University of Limoges, Limoges, France, in 1990. He is currently a Professor with the University of Limoges and Member of XLIM Research Institute, University of Limoges/National Center for Scientific Research (CNRS), Brive, France. His research interests include ultrawideband metrology for various applications, radar, EMCs, and HPMs.

Vincent Couderc received the Ph.D. degree from the University of Limoges, Limoges, France. He is currently the Head of the Photonics Group, XLIM Research Institute, Limoges, France. His research interests include spatial solitons propagation, diode-pumped laser source, nonlinear frequency conversion, and optoelectronic switching. Dr. Couderc is a member of the French Optical Society.

Badr M. Shalaby received the Ph.D. degree from the Université de Limoges, Limoges, France, in 2011. He is currently a Lecturer with the Physics Department, Faculty of Science, Tanta University, Tanta, Egypt, and also holds a post-doctoral position with the Photonics Group, XLIM Research Institute, Université de Limoges. His current research interests include semiconductor, optical fiber laser, diode pumped laser source, nonlinear frequency conversion, and optoelectronic switching. Dr. Shalaby is a member of the French Optical Society.

Laurent Pécastaing received the Ph.D. degree and the Research Directorship Habilitation degree in electrical engineering from the Université de Pau et des Pays de l'Adour (UPPA), Pau, France, in 2001 and 2010, respectively. He is currently an Associate Professor and the Head of the Electrical Engineering Team with the SIAME Laboratory, UPPA. His current research interests include high-power microwave sources and compact pulsed power devices, including pulse-forming lines, pulse transformers or Marx generators, and ultrafast transient probes.

Antoine Silvestre De Ferron was born in Tarbes, France, in 1977. He received the Ph.D. degree in electrical engineering from the Université de Pau et des Pays de l'Adour (UPPA), Pau, France, in 2006. He was a Researcher with the Atomic Energy Commission, Le Barp, France, from 2006 to 2008, which is a French government-funded technological research organization. He is currently an Engineer with the SIAME Laboratory, UPPA. His current research interests include high pulsed power generation for military and civil applications and combined high-voltage transient probes.

Laurent Desrumaux was born in St-Priest, France, in 1985. He received the Ph.D. degree in electronics from the University of Limoges, Limoges, France, in 2011. He is currently an Engineer with the DGA (French armament procurement agency), Paris, France. His research interests include ultrawideband RADAR systems and electronic warfare.

https://doi.org/10.1017/S1759078716000684 Published online by Cambridge University Press